UNIVERSIDADE DE SÃO PAULO

INSTITUTO DE FÍSICA
CAIXA POSTAL 20516
01498 SÃO PAULO - SP
BRASIL

PUBLICAÇÕES

IFUSP/P-950

DATA-TO-DATA RELATIONS FOR HEAVY ION EXCITATION OF GIANT RESONANCES AT INTERMEDIATE ENERGIES

Mahir S. Hussein
Instituto de Física, Universidade de São Paulo

Novembro/1991

DATA–TO–DATA RELATIONS FOR HEAVY ION EXCITATION OF GIANT RESONANCES AT INTERMEDIATE ENERGIES*

Mahir S. Hussein

Nuclear Theory and Elementary Particle Phenomenology Group
Instituto de Física, Universidade de São Paulo
C.P. 20516, 01498, São Paulo, S.P., Brazil
E–mail: HUSSEIN @ USPIF1.Bitnet
FAX: (55)(11) 814–0503

[Invited Talk at the Notre Dame Workshop on Giant Resonances and Related Phenomena, October 21–23, 1991, Notre Dame, Indiana, USA]

Abstract

It is shown that within a Glauber–DWBA description of the heavy–ion inelastic xcitation of giant resonances at intermediate energies, simple data–to–data (DTD) elations that relate the cross–section of these excitations to the elastic angular istribution, can be derived. Within the angular region where the DTD relations hold, the greement with the data on the GDR and GQR in the reaction $^{17}O + ^{208}Pb$ at $_{Lab} = 84$ MeV.A is remarkable.

---

* Supported in part by CNPq

November/1991

I. Introduction

Recently the experimental study of the formation and decay of giant resonances in the reaction $^{17}O + ^{208}Pb$ at $E_{Lab} = 84$ MeV.A has been reported by Bertrand et al.[1]. This study, as well as others on GR excitation with intermediate energy heavy ions, opens the possibility of a detailed investigation of the multipolarity content, relative strength, decay branching ratios and other aspects of the highly collective nuclear states. Usually, the data are successfully analysed with appropriate DWBA codes[2], and related formalisms[3]. A complicating feature of the analysis is the presence of strong nuclear effects, which renders the investigation of the GR more model dependent, as compared to the case of pure Coulomb excitation.

The thrust of this paper is to show that the presence of both strong Coulomb and nuclear interactions in the scattering of heavy ions allows the derivation of simple data–to–data (DTD) relations that connects the inelastic cross–sections to the elastic angular distribution[4]. This is made possible owing to the dominance, at the small angles where data are available, of Coulomb rainbow (CR) scattering. On the dark side of the CR no Coulomb–nuclear interference is present owing to the existence in the elastic and inelastic amplitudes of only one complex stationary phase contribution. We present arguments that in this angular region the cross–section $\sigma^{\lambda}_{inel}(q)$ for the excitation of a giant resonance of multipolarity λ, behaves as $C_{\lambda}\, q^2\, \sigma_{el}(q)$ where q is the momentum transfer and σ_{el} is the elastic angular distribution. The factor C_{λ} does not depend on q. Thus we propose that the $q^2\, \sigma_{el}(q)$ behaviour of $\sigma^{\lambda}_{inel}(q)$ in the dark side of the CR is universal and does not depend on λ. We base our analysis on DWBA with eikonal distorted waves.

We remind the reader that DTD relations have been derived and used previously by

Amado et al.[5] for proton–induced reactions in the 800 MeV range. The major difference between our work here and that of Ref. 5) is the strong Coulomb effects in our heavy–ion system.

II. The Data–to–Data Relations

Within the DWBA–einkonal theory, the inelastic amplitude for the excitation of giant multipole resonance (λm) is given by

$$F^{\lambda\mu}(q) = f_N^{\lambda\mu}(q) + f_C^{\lambda\mu}(q) \tag{1}$$

where the nuclear, $f_N^{\lambda\mu}$ and Coulomb, $f_C^{\lambda\mu}(q)$ components are given by

$$f_{N,C}^{\lambda\mu}(\theta) = \frac{ik}{2\pi\hbar v}\int e^{i\vec{q}\cdot\vec{r}+i\chi(b)} \left\langle \vec{r},\lambda\mu \middle| U_{N,C} \middle| \vec{r},0 \right\rangle d\vec{b}\, dz \tag{2}$$

where $\vec{r} = (\vec{b},z)$.

In (2) the eikoned fase $\chi(b)$ is given by

$$\chi(b) = -\frac{k}{E}\int_{-\infty}^{\infty} \left[U_N\left(\sqrt{b^2+z^2}\right) + U_C\left(\sqrt{b^2+z^2}\right)\right] dz \tag{3}$$

where the optical potential $U_N\left(\sqrt{b^2+z^2}\right)$ is the ground state expectation value of U_N of Eq.(2), and U_C is the Coulomb interaction between the two ions.

To set the stage for our DTD analysis we compare Eq.(2) to the elastic amplitude

given by

$$f_{el}(q) = \frac{ik}{2\pi}\int e^{i\vec{q}\cdot\vec{r}}\left[1 - e^{i\chi(b)}\right] d\vec{b}\, dz = ik\int\left[1 - e^{i\chi(b)}\right] J_0(qb)\, db \ . \tag{4}$$

If the small q region is avoided, the factor 1 inside the square brackets may be ignored and a straightforward comparison with Eq.(2) can be made. Recognizing that the matrix element $\langle \vec{r},\lambda\mu | U_N | \vec{r},0 \rangle$ is related to the derivation of the spherical optical potential, and ignoring e^{iqz} in line with the eikoned approximation one can immediately see that the z–integral in (2) can be related to $\chi(b)$ and its derivatives with respect to b . Thus through integration by parts the integral in (2) comes out proportional to $q\, f_{el}(q)$ irrespective to the multipolarity.

We now turn to a detailed analysis of the problem. First, we evaluate the elastic scattering amplitude and assess the nature of the process. We use the "$t_{\rho\rho}$" model for the nuclear optical potential, taking full account of medium effects on the nucleon–nucleon t–matrix[6]. After employing a Gaussian approximation for the densities of the projectile and target, which is reasonable owing to the surface nature of the excitation (see Fig. 1), we obtain for the nuclear phase $\chi_N(b)$, the following

$$\chi_N(b) = -\pi^2\frac{k}{E}\langle t_{NN}\rangle \frac{\alpha_1^3\ \alpha_2^3}{\alpha^2}\ \rho_{G,1}\ \rho_{G,2}\ e^{-b^2/\alpha^2} \tag{5}$$

where $\alpha^2 = \alpha_1^2 + \alpha_2^2$, $\rho_i(r) = \rho_{G,i}\, e^{-r^2/\alpha_i^2}$, $t_{NN} = -\frac{1}{2} i\hbar v\, \sigma_{NN}(E)\, [1-\alpha_{NN}(E)]$. The parameters relevant at 84 MeV.A are $\sigma_{NN} = 50$ mb, $\alpha_{NN} = 1$, $\alpha_i = \sqrt{2\alpha R_i}$, $\rho_{G,i} = 1/2\, \rho_0\, e^{R_i/2\alpha}$, $\rho_0 = 0.17\ fm^{-3}$, $\alpha = 0.65$ and $R_i = 1.2\ A_i^{1/3}$ fm . The comparison to the elastic scattering data of Barrette et al.[7], is shown in Fig.(1). It is obvious that our eikonal calculation of $\sigma_{el}(q)$ is quite good.

More insight can be gained if one performs a near/far decomposition of the elastic amplitude (and cross–section)[8]. This is accomplished by employing the following decomposition of the Bessel function

$$J_0(qb) = \frac{1}{2}\left[H_0^{(1)}(qb) + H_0^{(2)}(qb)\right] \tag{6}$$

where $H_0^{1(2)}(qb)$ are Hankel functions of zero order of the first and second type, respectively. Asymptotically these functions behave as

$$H_0^{1(2)}(x) \xrightarrow[x\gg1]{} \left[\frac{2}{\pi x}\right]^{1/2} \exp\left[+(-)i\left[x - \frac{\pi}{4}\right]\right] . \tag{7}$$

The amplitude, $f_{el}(q)$ can then be written as a sum of two contributions

$$f_{el}(q) = f_{el}^{Near}(q) + f_{el}^{Far}(q) \tag{8}$$

where f_{el}^{Near} is obtained from by replacing J_0 by $1/2\, H_0^{(2)}(qb)$ and f_{el}^{Far} by replacing J_0 by $1/2\, H_0^{(1)}(qb)$. In fig.(2) we show the contributions of f^{Near} and $f^{Far}(q)$ to the cross section. It is clear that in the angle range $0 < \theta < 6^o$, the cross section is completely near side dominated.

Since the product qb in the surface region is rather large, one can use the asymptotic form of $H_0^{1(2)}$, Eq.(7), to evaluate f_{el}^{Near} and f_{el}^{Far} within the stationary phase approximation. These solutions are obtained from the condition $d/db\,(\mp qb + \chi(b)) = 0$ or

$$\pm q = \frac{d}{db}\chi(b)\Big|_{b_{N(F)}} \equiv q(b) . \tag{9}$$

The function $q(b)$ is called the momentum transfer function and was introduced in Ref.(9). It is the Glauber analog of the WKB–based classical deflection function.

In fig.(3) we show $q(b)$ vs b for the $^{17}O + {}^{208}Pb$ system at $E_{Lab} = 84$ MeV.A . It is clear that two stationary phase solutions contribute to $f_{Near}(q)$ at $q < q_r = 1.86^{-1}$fm , the Coulomb rainbow transfer. The far–side amplitude, f_{Far}, much smaller, may contain two–stationary phase contributions, since $q(b)$ exhibits also nuclear rainbow at large negative values of $q(b)$. However, the inner contribution should be even more damped due to absorption. We concentrate now on $f_{Near}(q)$. Calling the two stationary phase impact parameters, b_1 and b_2 ($b_1 < b_r$, $b_2 < b_r$, $b_r = 11.7$ fm) the near–side amplitude $f_{el}^{Near}(q)$ can be easily evaluated and we find, using the primitive semiclassical approximation,

$$f_{el}^{Near}(q) = \frac{-ik}{2}\sqrt{\frac{2}{\pi q}}\, b_1^{1/2}(q)\sqrt{\frac{2\pi i}{\chi''(b_1)}}\; e^{i\chi(b_1(q)) - iq\, b_1(q)} + \frac{-ik}{2}\sqrt{\frac{2}{\pi q}}\, b_2^{1/2}(q)\sqrt{\frac{2\pi i}{-|\chi''(b_2)|}}\; e^{i\chi(b_2(q)) - iq\, b_2(q)} . \tag{10}$$

Note that $\chi''(b_2) \equiv q'(b_2)$ is negative (see fig.(3)). Further, $|\chi''(b_1)| > |\chi''(b_2)|$. This makes the contribution of the second term (the Coulomb term) to be increasingly dominant as q is decreased. The oscillations seen in the elastic angular distribution in the angle range $0^0 < \theta < 2^0$ result from the interference between the two contributions to $f_{el}^{Near}(q)$ given in Eq.(10).

On the dark side of the Coulomb rainbow, $q > q_r = 1.86$ fm^{-1} ($\theta_r = 3.3^0$, $b_r = 11.5$ fm) only one complex stationary phase contributes. The imaginary part of b is such as to give an over all damping in the amplitude in this case is to use the Airy approximation[10], which gives, for $q > q_r$, the following

$$f_{el}^{Near}(q) = \frac{k}{\sqrt{q}}\, e^{-i\,\pi/4}\, (b_r - i\xi)^{1/2}\, \frac{1}{\sqrt{\xi |q_r''|}}\, e^{-\frac{1}{3}\xi^3 |q_r''|}\, .$$

$$\cdot \exp\left[i\left(\chi_r - b_r\,\chi_r' - \frac{1}{2}\, b_r\, \xi^2\, \chi_r''\right)\right] \tag{11}$$

where $\xi = \sqrt{\frac{2(q-q_r)}{|q_r''|}}$ and it represents the imaginary part of the complex stationary point $\bar{b} = b_r - i\,\xi$. The subscript r refers to the rainbow, and $\xi_r \equiv \frac{d}{db}\chi(b)\Big|_{b=b_r}$ etc..

The cross–section q–dependence in the shadow region of the rainbow, then is given by

$$\frac{d\sigma}{d\Omega}(q > q_r) \simeq \frac{k^2}{q}\, b_r \left[\frac{1}{(|q_r''|)^{1/2}}\, \frac{e^{-\frac{2}{3}\left[\frac{2(q-q_r)}{|q_r''|^{1/3}}\right]^{3/2}}}{(2(q-q_r))^{1/2}}\right] , \tag{12}$$

which shows clearly the damping alluded to above, as one goes further inside the classically forbidden region.

II.b The Inelastic Amplitude

The inelastic scattering amplitude, Eq.(2) can be further simplified after integrating over the azimuthal angle $d\vec{b} = d\, db\, d\phi$. The we have, using the Tassie model[11]

$$f_{N,C}^{\lambda\mu}(q) = \frac{i^{1+\mu}\, C_\lambda\, k}{\hbar v} \int_0^{-\infty} b\, db\, J_\mu(qb)\, e^{i\chi(b)} \int_\infty^{-\infty} dz\, r^\lambda\, U_{N,C(\lambda)}\left(\sqrt{b^2+z^2}\right) P_{\lambda\mu}(\theta) \tag{13}$$

where $\sin\theta = \frac{b}{r}$ and $r^2 = b^2 + z^2$. The Coulomb interaction with $C(\lambda)$ means $\frac{1}{r^{2\lambda+1}}$ can be conveniently written as

$$P_{\lambda\mu}(\theta) = \frac{(-)^{\lambda+2|\mu|}}{2^\lambda\ \lambda!} \sqrt{\frac{(2\ell+1)(\ell+|\mu|)!}{4\pi(\ell-|\mu|)!}} \left[\frac{b}{\sqrt{z^2+b^2}}\right]^{-|\mu|} \left[\frac{(b^2+z^2)^{3/2}}{b^2}\right]^{\lambda-|\mu|} .$$

$$\cdot \frac{d^{\lambda-|\mu|}}{d\ z^{\lambda-|\mu|}} \left[\frac{b}{\sqrt{z^2+b^2}}\right]^{2\lambda} . \tag{14}$$

It is clear from the structure of Eq.(14) for $P_{\lambda\mu}(\theta)$, that the second integral in Eq.(13) can be written as a linear combination of $\chi_{N,C}(b)$ and their higher derivation whith respect to b. Let us call the z integral $F_{N,C(\lambda)}^{\lambda\mu}(b)$. Thus, with the asymptotic form of $J_\mu(qb)$, which is valid since $qb \gtrsim 2(R_1+R_2)$,

$$J_\mu(qb) = \sqrt{\frac{2}{\pi qb}} \cos\left[qb - \mu\frac{\pi}{2} - \frac{\pi}{4}\right] ,$$

and considering only the near–side contribution, we have

$$F_{N,C}^{\lambda\mu}(b) = \frac{i^{1+\mu}\, C_\lambda\, k}{\hbar v} \sqrt{\frac{-i}{2q\pi}} \int_0^{-\infty} b^{1/2}\, F_{N,C(\lambda)}^{\lambda\mu}(b)\, db\, e^{i\chi(b)-iqb} . \tag{15}$$

Since $b^{1/2}\, F_{N,C(\lambda)}^{\lambda\mu}(b)$ varies slowly with b, one may evaluate the above integral employing the Airy approximation and we find in the shadow of the rainbow

$$f^{\lambda\mu}_{N,C}(q) \simeq \frac{-\, i^{1+\mu}\, C^{C,N}_{\lambda}}{\hbar v}\, F^{\lambda\mu}_{N,C(\lambda)}(\bar{b}(q))\; f^{Near}_{el}(q) \tag{16}$$

where $\bar{b}(q)$ is the complex stationary point impact parameter, given by $b_r - i\xi$ (see Eq. 11).

Eq. (16) is the basis of our data–to–data relations. We have applied the formalism above to the case of the isovector giant dipole resonance (IVGDR) and the isoscalar giant quadrupole resonance (ISGQR). The evaluation of the quantity $F^{\lambda\mu}_{N,C(\lambda)}(\bar{b}(q))$ is lengthy but straight forward[4,12]. We obtain the following forms for the cross–sections:

$$\sigma_{1^-}(q) \simeq \left|f^{1,1}_C(q)\right|^2 + \left|f^{1,-1}_C(q)\right|^2 = 2\left|f^{1,1}_C(q)\right|^2 = \frac{3}{4\pi}\left|\frac{C^C_1}{\eta}\right|^2 q^2\, \sigma_{el}(q) \tag{17}$$

where $\eta = \frac{z_1\, z_2\, e^2}{\hbar v}$ and $C_1 = \frac{\pi^{3/2}}{\sqrt{3}}\,\frac{z_p\, e^2}{\hbar v}\,\beta_1\, R_T\, \rho_{G,T}\, \alpha_T^3$. The deformation length

$$\beta_1\, R_T = \left[\frac{\pi\, N_T\, z_T\, \hbar^2}{2\, A_T\, m_N\, E^1_x}\right]^{1/2}, \text{ and}$$

$$\sigma_{2^+}(q) = 2\left|f^{2,2}_N\right|^2 + \left|f^{2,0}_N\right|^2$$

$$\sigma_{2^+}(q) = \frac{5}{64\pi}\left|C^N_1\right|^2 q^2\, b_r^2\, \sigma_{el}(q) \tag{18}$$

$$C^N_2 = \frac{2\pi^{3/2}}{\sqrt{5}}\,\beta_2\,\frac{\alpha^{12}}{\alpha_p^7\,\alpha_T^5} \quad\text{and}\quad \beta_1\, R_T = \left[\frac{20\,\pi\,\hbar^2}{3\, A_T\, m_N\, E^{2^+}_x}\right]^{1/2}.$$

In deriving (17) we have taken the modified–Coulomb amplitude $f^{11}_C(q)$ as to be dominant, which is reasonable for the isovector dipole excitation. In contrast, Eq. (18) was obtained assuming pure nuclear excitation. Clearly improvements can be made sincethe general amplitude

$$f^{\lambda\mu}(q) = f^{\lambda\mu}_N(q) + f^{\lambda\mu}_C(q) = \frac{-i^{\,1+\mu}}{\hbar v}\left[\, C^N_\lambda\, F^{\lambda,\mu}_N(\bar{b}(q)) + C^C_\lambda\, F^{\lambda,\mu}_{C(\lambda)}(\bar{b}(q))\,\right]\cdot$$

$$\cdot\, f^{Near}_{el}(q)\ ,\quad q > q_r\ . \tag{19}$$

In figure 4 and 5, we show our results based on Eqs. (17) and (18). The data are from Ref. 7). The elastic data are shown in Fig 1. Notice that the deformation lengths $\beta_1 R_T = 0.42$ fm and $\beta_2 R_T = 0.55$ fm used in our calculation are the same as those used in the DWBA–based calculation of Ref. 3. Thus the data–to–data relations, within the angular region where they hold $(q > q_r)$, seem to work remarkably well.

III. Conclusions and Discussion

We have derived DTD relations for the excitation of GR's in the heavy ion reactions at intermediate energies. The region of velocity of our DTD relations is the dark side of the Coulomb rainbow when no interference effects are present. Applications of our relations to the excitation of the IVGDR and the ISGQR in the $^{17}O + {}^{208}Pb$ reaction at 84 MeV/A is very good. Improvement upon the approximations employed and further application to other systems and GR's will be reported later.

References

1) See, e.g., F.E. Bertrand, J.R. Beene and D.J. Horen, *Nucl. Phys.* **A488** (1988) 163c.
2) G.R. Satchler, *Nucl. Phys.* **A472** (1987) 215.
3) A.N.F. Aleixo and C.A. Bertulani, *Nucl. Phys.* **A528** (1991) 436.
4) A.N.F. Aleixo, C.A. Bertulani and M.S. Hussein, to be published.
5) R.D. Amado, F. Lenz, J.A. McNeil and D.A. Sparrow, *Phys. Rev.* **C22** (1980) 2094.
6) A.K. Kerman, H. McManus and R.M. Thaler, *Ann. of Phys.* (NY) 8 (1959) 551; M.S. Hussein, R.A. Rego and C.A. Bertulani, *Phys. Rep.* **201** (1991) 279.
7) J. Barrete et al., *Phys. Lett.* **B209** (1988) 182.
8) M.S. Hussein and K.W. McVoy, *Prog. Part. Nucl. Phys.* **12** (1984) 103.
9) B.V. Carlson, M.P. Isidro Filho and M.S. Hussein, *Phys. Lett.* **B154** (1985) 89.
10) M.P. Pato and M.S. Hussein, *Phys. Rep.* **189** (1990) 127.
11) L.J. Tassie, *Austral. J. Phys.* **9** (1956) 407.
12) M.S. Hussein, to be published.

Figure Captions

Fig. 1. Elastic cross section data for the system $^{17}O + {}^{208}Pb$ at 84 MeV/nucleon. Data are from ref. 7. The solid curve is our theoretical prediction.

Fig. 2. The Near–side and Far–side contributions for the elastic angular distribution. (See text for details).

Fig. 3. The momentum transfer function $q(b)$ versus b. See text for details.

Fig. 4. Cross section for the excitation of isovector giant dipole resonance. Data are from ref. 7. The solid curve was obtained from the data–to–data relation given by eqs. (6) and (8), with deformation parameter $\beta_1 R = 0.42$ fm .

Fig. 5. The same as in fig. 3, but for the isoscalar giant quadrupole resonance. We used here $\beta_1 R = 0.55$ fm .

Near - Far decomposition

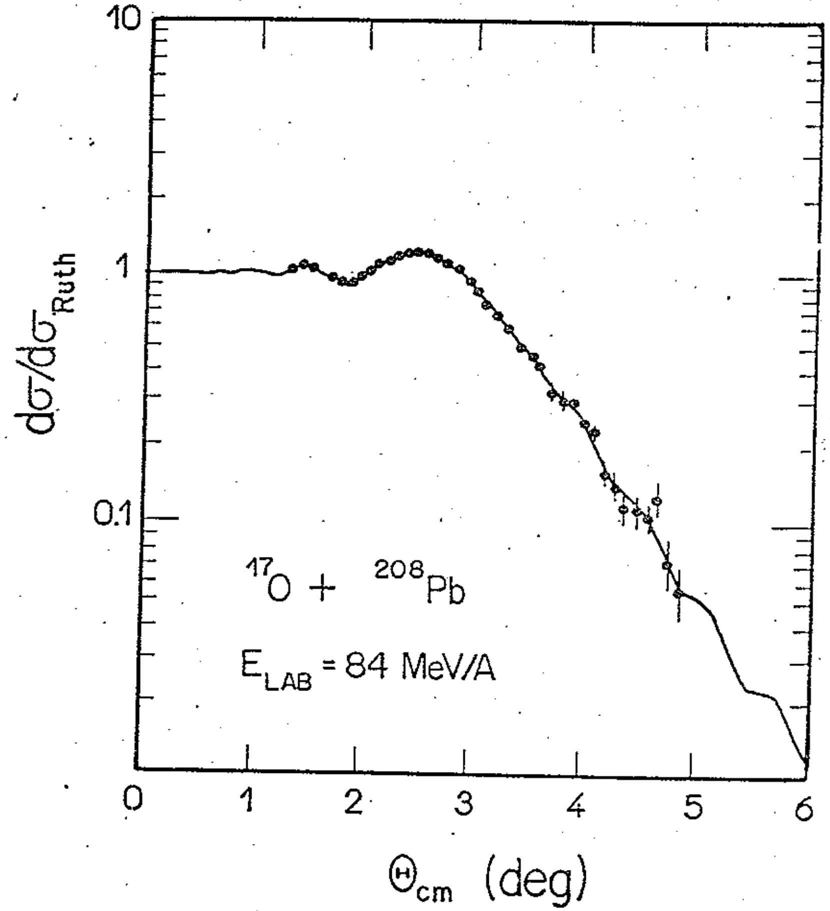

Fig. 1

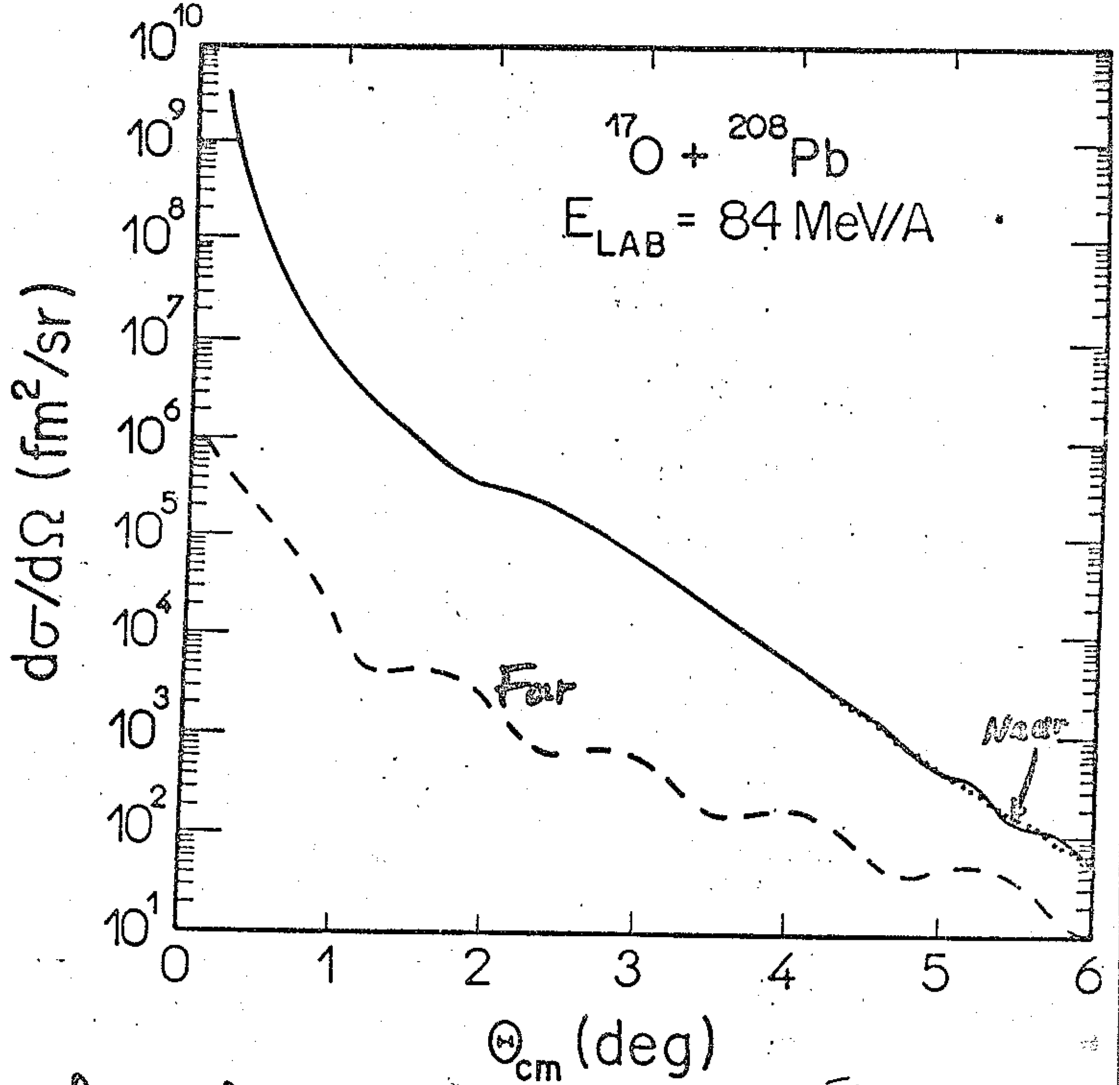

Fig. 2

$$f_{el} = f_{Near} + f_{Far}$$

$$f_{\substack{Near \\ FAR}} = \frac{-ik}{2}\int_0^\infty db\, b\, H^{\frac{1}{2}}(qb)\left(e^{i\chi(b)} - 1\right)$$

$$H^{1\{\frac{2}{x}\}} \longrightarrow \left(\frac{2}{\pi x}\right)^{1/2} \exp\left(+(-)\, i\left(x - \frac{\pi}{4}\right)\right)$$

Momentum Transfer Function
q(b) ["deflection function"]

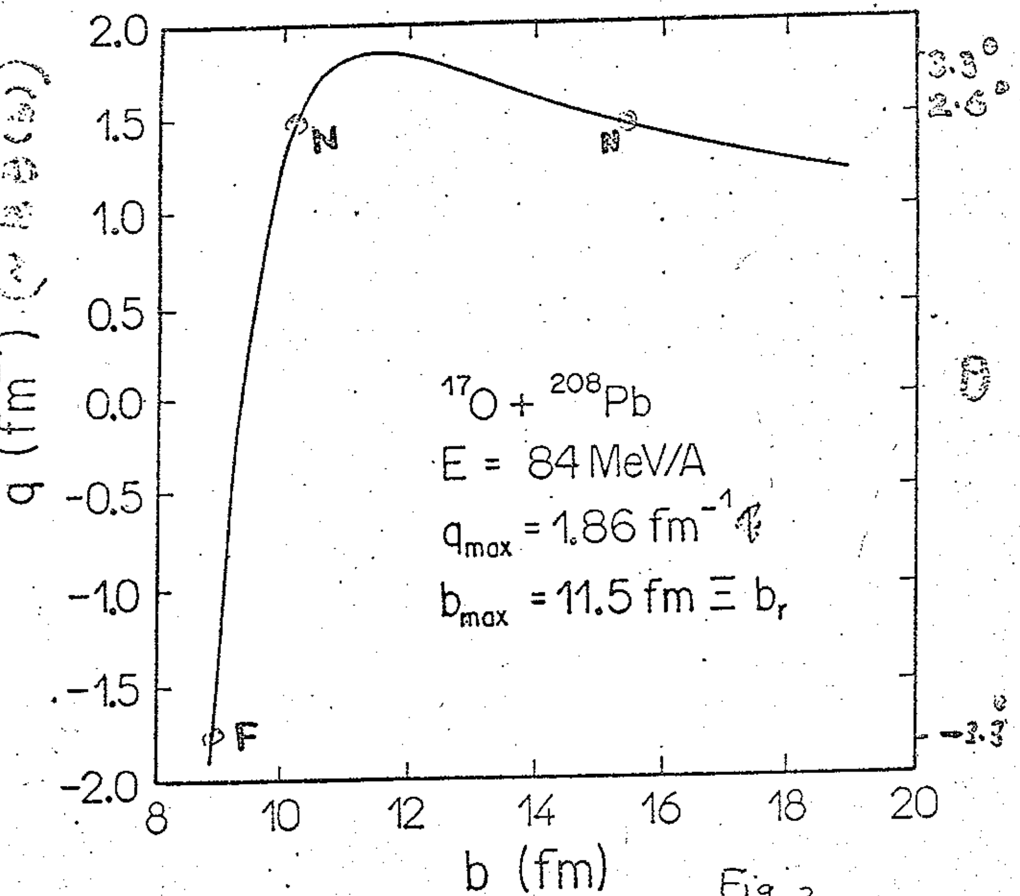

Fig. 3

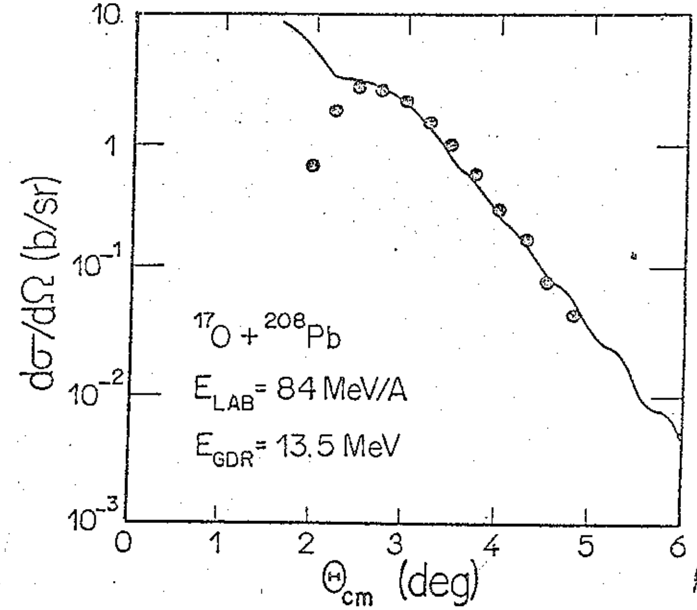

Fig. 4

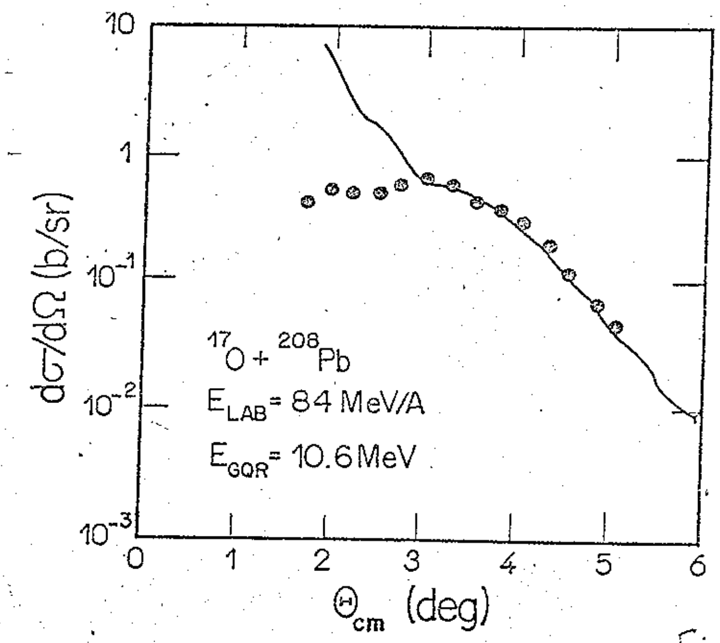

Fig. 5